Journal of Hydrology: Regional Studies 37 (2021) 100878

Contents lists available at ScienceDirect

Journal of Hydrology: Regional Studies

journal homepage: www.elsevier.com/locate/ejrh

Isotopic constraints on water balance and evapotranspiration partitioning in gauged watersheds across Canada

J.J. Gibson [a,b,*], T. Holmes [c,d], T.A. Stadnyk [c,d], S.J. Birks [b,e], P. Eby [a], A. Pietroniro [f]

[a] InnoTech Alberta, 3-4476 Markham Street, Victoria, BC V8Z 7X8, Canada
[b] University of Victoria, Geography, Victoria, BC V8W 3R4, Canada
[c] University of Calgary, Geography, Calgary, AB T2N 1N4, Canada
[d] University of Manitoba, Civil Engineering, Winnipeg, MB R3T 5V6, Canada
[e] InnoTech Alberta, 3608 - 33 St NW, Calgary, Alberta T2L 2A6, Canada
[f] National Hydrological Service, Meteorological Service of Canada, National Hydrology Research Centre, 11 Innovation Blvd., Saskatoon, SK S7N 3H5, Canada

ARTICLE INFO

Keywords:
Stable isotopes
Vapour partitioning
Rivers
Evaporation
Transpiration
Runoff

ABSTRACT

Study region: During 2013–2019, we conducted a Canada-wide program of streamflow sampling for the analysis of stable isotopic composition ($^{18}O/^{16}O$ and $^{2}H/^{1}H$), providing the first comprehensive survey for gauged watersheds across Canada ranging from 10 to 10,000 km^2. A watershed-based assessment of vapour and runoff partitioning is presented for 103 watersheds across a diverse range of climate and land cover types, spanning 25° latitude and 86° longitude.
Study focus: An isotope-based methodology is applied to estimate evaporation/inflow (E/I) and transpiration/evapotranspiration (T/ET) utilizing offset between isotope values in streamflow and precipitation, augmented by regional climate reanalysis data. Isotopic enrichment in streamflow serves to differentiate direct, abiotic evaporation, mainly arising from open water evaporation from lakes and wetlands, from transpiration by natural vegetation and cropland, which has previously been recognized as principally non-fractionating. Sensitivity analysis suggests only a minor influence of interception losses on T/ET.
New hydrological insights for the region: Systematic variations in evaporation losses, transpiration losses and gauged runoff are revealed across the major hydrometric regions of Canada. Calculations suggest that E/I ranged from 2 to 60 %, while T/ET ranged from 25 to greater than 95 % across the watersheds. A new water loss classification is introduced which reveals that 19 of 103 watersheds were runoff-dominated, 54 were transpiration-dominated, 5 were evaporation-dominated, and 27 had more than one dominant water loss mechanism.

1. Introduction

A stable isotope (^{18}O and ^{2}H) survey of river discharge across Canada was recently conducted as part of a multi-year monitoring program operated by the Water Survey of Canada during 2013–2019 (Gibson et al., 2020, 2021). Similar programs carried out previously across the United States (Kendall and Coplen, 2001), Europe (Rank et al., 1998; Koeniger et al., 2009; Reckhert et al., 2017) and worldwide, as part of the Global Network of Isotopes in Rivers (Gibson et al., 2002a; Vitvar et al., 2007; Halder et al., 2015) have

* Corresponding author at: InnoTech Alberta, 3-4476 Markham Street, Victoria, BC V8Z 7X8, Canada.
E-mail address: jjgibson@uvic.ca (J.J. Gibson).

https://doi.org/10.1016/j.ejrh.2021.100878
Received 27 January 2021; Received in revised form 16 July 2021; Accepted 20 July 2021
Available online 30 July 2021

sought to exploit the capabilities of isotopes for tracing dynamics of water source contributions such as rain, snow, soil water, groundwater, lakes, wetlands, and glacier ice, in meso-scale to large-scale watersheds (e.g. Gibson et al., 2016a; Ala-aho et al., 2018; Kumar et al., 2018). Previous studies have also effectively applied isotopes for assessment of water balance (Gibson et al., 1993; Gibson, 2001; Gibson and Edwards, 2002; Henderson-Sellers et al., 2004; Gibson and Reid, 2010, 2014), groundwater mixing during snowmelt or storm events (St. Amour et al., 2005; Klaus and McDonnell, 2013), quantification of groundwater connectivity to rivers (Stadnyk et al., 2015; Koeniger et al., 2009), flowpath tracing and estimation of water residence times (Rodgers et al., 2005; McGuire and McDonnell, 2006), detection of recharge bias (Jasechko et al., 2017), estimating young water fractions in streamflow (Kirchner, 2016; Jasechko et al., 2016; Allen et al., 2017), and validation of distributed hydrological models (Fekete et al., 2006; Stadnyk et al., 2013, 2015; Smith et al., 2015, 2016; Belachew et al., 2016; Stadnyk and Holmes, 2020). The Canadian rivers dataset is significant in that it extends the 221 station GNIR network of Halder et al. (2015) by an additional 331 stations, including many representative cold regions watersheds with mean annual temperatures ranging from +7 to −7 °C.

One of the prevalent isotopic signals noted in river discharge across Canada is evaporation, often immediately detected when data are plotted in δ^{18}O-δ^{2}H space owing to isotopic signatures that fall below the meteoric water line (Gibson et al., 2020). The evaporation process is known to cause isotopic enrichment of heavy isotopic species in the residual liquid, due to the less energetic behaviour of the heavy isotopic species (i.e. isotopologues, $^{1}H^{1}H^{18}O$, $^{1}H^{2}H^{16}O$) during diffusion across the air-water interface (Horita et al., 2008). Evaporation may occur as water flows along river channels (Gremillion and Wanielista, 2000; Gibson et al., 2008a), although such influences are often subordinate to evaporative signals inherited from lakes and wetlands residing within the watershed, as these water bodies typically have much longer residence times and cover a higher percentages of surface area within the catchment (Gibson and Edwards, 2002; Gibson et al., 2016a). Evaporation is also enhanced progressively along chain-of-lakes drainage systems (e.g. Gibson and Reid, 2014), which are prevalent in 48 % of Canada's landmass underlain by crystalline Precambrian Shield bedrock. Previous studies in arid climate zones have also shown appreciable evaporative enrichment of heavy isotopic species in soil porewaters, although such labelling is often realized only in dry, bare soils (Allison et al., 1983; Barnes and Allison, 1988). Dry, bare soil areas are most often disconnected or intermittently connected to river networks, and presumably are less likely to be a sustained or prevalent source of heavy-isotope enriched water in river discharge (Gibson et al., 2008b). Here, we apply isotopic enrichment in streamflow to better understand the underlying mechanisms associated with vapour loss across a broad range of climate zones within Canada, utilizing the newly available ^{18}O and ^{2}H dataset as compared to precipitation isotope data and recent Canadian isoscape modelling efforts (Delavau et al., 2015).

Vapour loss mechanisms, including canopy interception, evaporation from soil, evaporation from wet surfaces, and transpiration by plants, are often referred to collectively as evapotranspiration (ET), a key component of the global water cycle regulating both atmospheric and surface water balance on the continents (Li et al., 2019). As coupling of the water and carbon cycles by CO_2 uptake and vapour release during photosynthesis is linked only to plant-mediated transpiration (Telmer and Veizer, 2000), a number of ecohydrology studies have proposed significant advantages for independent characterization or separation of transpiration from the bulk evapotranspiration flux, including better understanding of responses to individual drivers (Schleisinger and Jasechko, 2014). Several advantages include validation and improvement of ecosystem models (Shichun et al., 2010; Sutanto et al., 2012; Li et al., 2019), application of water use efficiency based on transpiration estimates to calculate net primary productivity (Telmer and Veizer, 2000; Mastrotheodoros et al., 2017), ability to track stomatal response to environmental stressors (Li et al., 2019), and overall, for better understanding of land-atmospheric interactions related to land use, drought and climate change (Berg and Sheffield, 2019).

Several techniques employed for ET partitioning at the plot- to ecosystem-scale include stable isotope methods, sap flow, eddy-covariance, and modelling. Isotope-based methods make use of the fact that evaporation and transpiration differently fractionate the stable isotopes of water (Kool et al., 2014) although they may be costly and labour intensive, often requiring diurnal leaf water measurements. Watershed-based partitioning of evaporation and transpiration relying on isotopic enrichment in river discharge has also been employed, as was initially demonstrated by Gibson et al. (1993) and subsequently applied in a number of large river basin studies (Telmer and Veizer, 2000; Lee and Veizer, 2003; Ferguson et al., 2007). Notably, Ferguson and Veizer (2007) show a comparison of results for 15 large watersheds in the Americas, Africa, Australia and New Guinea including discussion of implications for the net primary productivity and the global carbon cycle. An informative review of the approach within the context of global water and carbon cycle research is provided by Schulte et al. (2011). Jasechko et al. (2013) extended application of the method to partition evapotranspiration for 73 large lake basins, thereby assembling a perspective on the global significance of transpiration for land surfaces. While Jasechko et al. (2013) concluded that transpiration may account for 80–90 % of global evapotranspiration from the continents, this assertion was subsequently challenged based on contentions regarding uncertainty propagation of the method (Coenders-Gerrits et al., 2014), uncertainties regarding global interception estimates (Coenders-Gerrits et al., 2014, Schleisinger and Jasechko, 2014), as well as representativeness of applying lake isotopic signals to represent entire catchment areas, owing to hydrological decoupling (Schlaepfer et al., 2014). While representativeness plays a deterministic role in all isotope-based investigations, particularly at the large scale, many other criticisms of the method have since been rebuked or explained (Jasechko et al., 2014a). Nevertheless, recent field scale tests of the method have shown more optimistic results (Hu et al., 2018).

In extending a similar approach to watersheds situated in 10 hydrometric regions across Canada, we illustrate refinements in methodology and implications of systematic variations across a range of hydroclimatic conditions for watersheds draining to the Atlantic, Pacific and Arctic Oceans. Overall, our hypothesis is that extent of open water and wetlands in watersheds will be the dominant drivers of evaporation losses, whereas forest cover type and cropland will be the dominant driver of transpiration losses. The main objectives of this paper are to evaluate a watershed-based isotope mass balance approach for characterizing vapour partitioning mechanisms in a diverse range of hydrological regimes across Canada, to evaluate systematic influence of land cover characteristics on vapour partitioning mechanisms, and to demonstrate a novel classification framework for watersheds based on dominant water loss mechanisms. Challenges, limitations and implications for future research and monitoring in Canada are also discussed.

2. Methods

2.1. Study sites

Of 331 gauging stations within the isotope sampling program operated by Water Survey of Canada, 162 stations met our criteria to enable reliable estimation of flow weighted isotopic compositions (see Gibson et al., 2020, 2021). A total of 103 of these stations were used in the vapour partitioning (VP) analysis presented here (Table 1, Fig. 1). For these VP stations, streamflow was found to be heavy-isotope enriched relative to long-term precipitation, and so were amenable to a first-order quantification of evaporation losses using a simple, analytical isotope enrichment model. The remainder of stations (61) were not used in this preliminary assessment owing to: (i) significant content of water sources in streamflow other than modern precipitation (i.e., glacier melt, glaciogenic groundwater reflux, or permafrost thaw), (ii) uncertainty in the prediction or interpolation of long-term precipitation isotope values for some remote or poorly monitored areas, and/or (iii) long residence times or storage lag effects in some watersheds resulting in a disconnect between the precipitation isotope input and streamflow response.

2.2. Isotope composition of streamflow

Oxygen-18 (^{18}O) and deuterium (^{2}H) isotopic composition of streamflow was determined from measurement of water samples collected at flow gauging stations operated by the Water Survey of Canada. Details of the streamflow network and sampling protocols have been described previously (Gibson et al., 2020, 2021). Water samples were analyzed using a Thermo Scientific Delta V Advantage isotope ratio mass spectrometer. Oxygen and hydrogen isotopes were analyzed on separate subsamples, with oxygen determined by equilibration using a Gasbench (Paul and Skrzypek, 2006) and hydrogen determined by injection of water on hot chromium using an H-Device reactor (Brand et al., 1996). Internal standards were selected that bracketed the dataset (i.e. δ^{18}O, δ^{2}H (‰): 1: −27.39, −213.6; 2: 3.88, −17.2; 3: −9.81, −72.1) Results are reported in "δ" notation in permil (‰) relative to Vienna Standard Mean Ocean Water (V-SMOW) and normalized to the SMOW-SLAP scale where SLAP is Standard Light Arctic Precipitation (Nelson, 2000). Analytical uncertainty predicted based on 2-σ of sample repeats is ±0.14 for δ^{18}O (n = 382) and ±0.52 for δ^{2}H (n = 450).

2.3. Climate data

Gridded (32-km) monthly climate data (1981–2001) including precipitation amount, evaporation amount, 2-m air temperature, and 2-m relative humidity were extracted from the North America Regional Reanalysis (NARR; Mesinger et al., 2006). Long-term basin-weighted values of climate parameters were obtained by averaging all grid-centered NARR datapoints falling within the specified watersheds of interest.

2.4. Isotopic characterization of precipitation, atmospheric water vapour and discharge

Isotopic composition of precipitation was estimated from time-series ensembles (2013–2019) using a modified version of the model of Delavau et al. (2015) that included δ^{2}H for all North American Regional Reanalysis (NARR) coordinates falling within the Canadian landmass, from which climate data were extracted. The regression-based model relies mainly on monthly data collected within the Canadian Network for Isotopes in Precipitation (CNIP) (Birks and Gibson, 2009), the United States Network for Isotopes in Precipitation (USNIP) (Welker, 2012) and Global Network for Isotopes in Precipitation (GNIP) (IAEA/WMO, 2014). Amount-weighted annual

Table 1
Summary of isotope monitoring by hydrometric region (modified after Gibson et al. (2020).

	Region	Analyses to date	Stations			Land area (km^2)	% Land Area monitored
			All	FW*	VP+		
1	Maritime	355	27	10	3	163,990	45.8
2	St. Lawrence	382	37	10	4	1,067,879	92.1
3	N. Quebec and Labrador	147	19	4	4	1,158,292	33.8
4	Southwestern Hudson Bay	291	25	8	8	735,320	92.7
5	Nelson River	1202	80	49	38	987,015	98.1 96.0
6	Western and Northern Hudson Bay	272	23	9	9	1,253,213	99.1
7	Great Slave Lake	622	45	24	15	974,853	95.0
8	Pacific	507	24	20	9	666,349	96.5
9	Yukon River	157	7	5	4	337,036	91.6
10	Arctic	668	44	23	9	2,605,138	46.0
11	Mississippi	0	0	0	0	27,097	0
	Unclassified (Marine Estuaries)	0	0	0	0	8486	0
	Total	4603	331	161	103	9,984,670	55.8

[*] Flow-weighted network stations.

[+] Vapour-partitioning network.

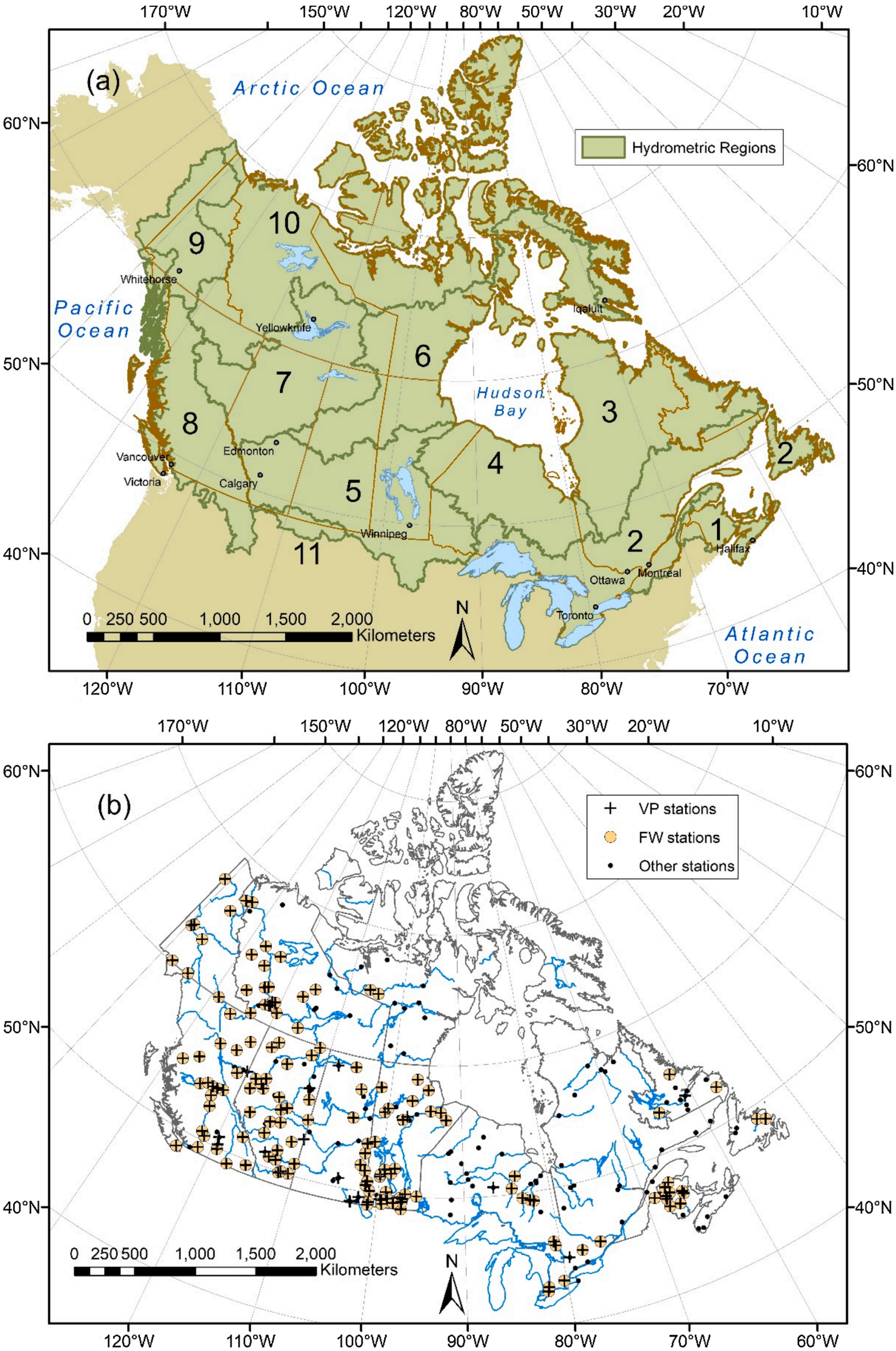

(caption on next page)

Fig. 1. Maps of Canada showing (a) hydrometric regions (after Gibson et al., 2020), (b) streamflow sampling stations by type, including sites used for vapour partitioning (E/I sites). See Table 1 for region names.

values for $\delta^{18}O$ in precipitation were calculated as the dot product of the sequence of monthly isotopic values and precipitation amounts, divided by the total precipitation. Basin-weighted averages were calculated by arithmetically averaging all grid-centered NARR datapoints falling within a watershed.

Isotopic composition of atmospheric water vapour was estimated using the precipitation-equilibrium assumption (Gibson et al., 2008b):

$$\delta_A = (\delta_P - \varepsilon^+)/\alpha^+ \quad (‰) \tag{1}$$

where ε^+ (‰) is the equilibrium water-vapour isotope separation (Horita and Wesolowski, 1994), and α^+ (decimal notation) is the equilibrium isotopic fractionation, where these quantities are related by $\varepsilon^+ \cdot 10^{-3} = \alpha^+ - 1$. To account for seasonally variable conditions under which evaporation takes place, the exchange terms in Eq. (1) were evaluated on a monthly time step and evaporation-flux-weighted for each grid-centered NARR datapoint. This was calculated as the dot product of the sequence of monthly δ_A outputs from Eq. (1) and monthly evaporation, divided by the total evaporation. Similar calculations were made to calculate the effective annual evaporation temperature and relative humidity at 2-m atmospheric height for each grid-centered NARR datapoint. Basin-weighted parameters were then estimated by arithmetically averaging all NARR datapoints within a watershed of interest.

Isotope composition of discharge was flow-weighted and calculated as the dot product of the isotopic composition of $\delta^{18}O$ and instantaneous flow at the time of sampling, divided by the mean flow. An equivalent calculation was used to flow-weight δ^2H.

2.5. *Water yield, storage effects, and interception*

Annual water yields were calculated for each watershed based on daily flow gauging records and reflect the mean depth of gauged streamflow from the watersheds of interest. Due to the use of long-term average climatic and hydrologic parameters, watershed storage effects were assumed to approach zero. Interception estimates were obtained from the Global Land Evaporation Model (GLEAM version 3.1; www.GLEAM.eu; Miralles et al., 2010) and were basin-weighted according to the methodology used for the NARR datasets.

2.6. *Isotope mass balance*

The isotopic data from the VP stations (103 in total) were analyzed to estimate the fraction of water loss by evaporation (E/I) from the watersheds, and the transpired vapour fraction, i.e. transpiration/total evapotranspiration (T/ET). The methodology of Gibson et al. (2015, 2016b, 2017, 2018, 2019) was used in the calculations but was adapted to be suitable for application to watersheds rather than lakes. A similar approach, but with simplifications, was used by Ferguson et al. (2007) for the Great Plains region of North America, and by Gibson et al. (2002b, 2010) for lakes in western Canada.

Evaporation/inflow for the watersheds was estimated as follows:

$$E/I = (\delta_I - \delta_Q)/(\delta_E - \delta_Q) \quad \text{(dimensionless)} \tag{2}$$

where δ_I, δ_Q and δ_E are the isotopic compositions of inflow, streamflow and evaporate (‰), respectively; the latter evaluated from the Craig and Gordon (1965) model given by:

$$\delta_E = ((\delta_L - \varepsilon^+)/\alpha^+ - h\delta_A - \varepsilon_K)/\left(1 - h + 10^{-3} \cdot \varepsilon_K\right) \quad (‰) \tag{3}$$

where h is relative humidity (decimal fraction), δ_A is isotopic composition of atmospheric water vapour (‰), and ε_K is the kinetic isotopic separation (‰; see Horita et al., 2008). As noted by Gibson et al. (2016b), substitution of δ_E from Eq. (3) into Eq. (2) yields:

$$E/I = (\delta_L - \delta_I)/(m(\delta^* - \delta_L)) \quad \text{(dimensionless)} \tag{4}$$

where

$$m = \left(h - 10^{-3} \cdot (\varepsilon_K + \varepsilon^+/\alpha^+)\right)/\left(1 - h + 10^{-3} \cdot \varepsilon_K\right) \quad \text{(dimensionless)} \tag{5}$$

and

$$\delta* = (h\delta_A + \varepsilon_K + \varepsilon^+/\alpha^+)/\left(h - 10^{-3} \cdot (\varepsilon_K + \varepsilon^+/\alpha^+)\right) \quad (‰) \tag{6}$$

For headwater catchments or watersheds, we note that inflow and its isotopic composition can be approximated by precipitation and its isotopic composition, respectively. By substituting $\delta_I \approx \delta_P$ and $I \approx P$ in Eq. (4), we define E/I for a headwater catchment estimated using the isotopic approach (x) to be:

$$x = E/P = (\delta_L - \delta_P)/(m(\delta^* - \delta_L)) \quad \text{(dimensionless)} \tag{4a}$$

The water balance of a watershed (non-isotopic) assuming zero change in storage can also be represented by

$$P - N = E + T + Q \quad \text{(mm/yr)} \tag{7}$$

where P, N, E, T and Q are the precipitation, interception, evaporation, transpiration, and gauged discharge, respectively. Recognizing the following: (i) that $E + T = ET$, which we now define as evapotranspiration, (ii) by rearranging Eq. (7) we obtain $ET = P - N - Q$, (iii) by rearranging Eq. (7) we also obtain $T = P - N - Q - E$, and (iv) by substitution of $E = x \cdot P$ from Eq. (4a) we obtain an expression for the fraction of vapour loss by transpiration:

$$T/ET = [P - N - Q - x \cdot (P - N)]/[P - N - Q] \quad \text{(dimensionless)} \tag{8}$$

In considering the possible role of interception in modifying the T/ET, we also introduce and test a simplified version of the water balance equation for comparative purposes that neglects interception losses:

$$T/ET = [P - Q - x \cdot P]/[P - Q] \quad \text{(dimensionless)} \tag{9}$$

3. Results and discussion

3.1. Isotope characteristics of streamflow, precipitation and vapour

Streamflow and estimated precipitation isotopic compositions are illustrated in dual isotope space in relation to modelled isotopic composition of water vapour sources from the 103 vapour partitioning (VP) watersheds across Canada (Fig. 2). The locus of precipitation values for gauged basins closely resembles theCanadian Meteoric Water Line (CMWL; Gibson et al., 2005, 2020). Measured streamflow is shown to be typically heavy-isotope enriched relative to precipitation, falling below the CMWL (Fig. 2). Further description and discussion of river trend lines in ^{2}H-^{18}O space based on this Canadian streamflow dataset has been provided by Gibson et al. (2020).

The modelled isotopic values for atmospheric moisture based on the equilibrium model are depleted relative to precipitation, plotting ostensibly along a subparallel extension of the meteoric water line trend. The Craig and Gordon (1965) model, used to estimate the isotopic values of evaporate from both open water and soil, predicts values that plot above the meteoric water line along subparallel, imbricated clusters, while transpiration is expected to fall closer to values for precipitation assuming net non-fractionating biotic transfer of soil water. Evapotranspiration is approximated as a mixture of non-fractionated transpiration and open-water evaporation. The strong potential of isotopic labelling of vapour by evaporation from bare soils is an end member that may be important in localized agricultural areas under tillage or summer fallow (Jalota and Prihar, 1990), but likely accounts for negligible amounts of annual vapour exchange across most natural Canadian landscapes. Differential labelling of various vapour fluxes occurs

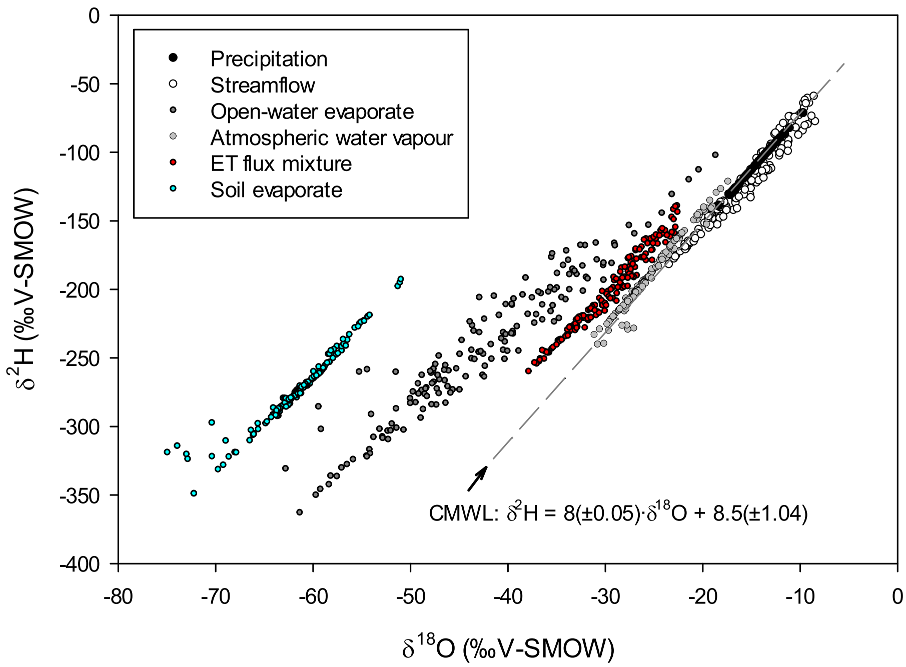

Fig. 2. Dual isotope plot showing measured isotopic composition of river water in relation to precipitation and estimated isotopic composition of atmospheric moisture, evaporate from open water, evaporation from soils, and simulated combined ET flux. Canadian Meteoric Water Line (CMWL) showing extent based on the observed monthly observations at Canadian stations.

due to variations in fractionation and mixing mechanisms. We note that reduced evaporation losses and reduced fractionation during liquid-vapour exchange is expected under conditions where large evaporating water bodies, such as large lakes, influence atmospheric water vapour in the boundary layer, and alter the isotopic composition of the overlying air mass in downwind areas. This effect has been described in detail from an isotope mass balance assessment of the Great Lakes (Jasechko et al., 2014b), and for smaller lakes located in coastal areas of Atlantic and Pacific coastal regions of Canada (Gibson et al., 2016b, 2018).

While our isotope balance calculations and the simulations shown in Fig. 2 assume that transpiration is non-fractionating over the long-term on the watershed scale, we acknowledge that non-mobile soil water compartments within the watershed (e.g. water held within soils below field capacity but above the wilting point) may also develop periodically, and may in some cases become a distinctly labelled source of transpired water, consistent with the two water worlds (TWW) hypothesis (McDonnell, 2014). The TWW concept, which remains to be widely tested (Evaristo et al., 2015), postulates that streams are fed by mobile soil water associated with infiltration and groundwater recharge, whereas plants may primarily be tapping into non-mobile soil water sources. Significant isotopic fractionation of non-mobile waters has been observed in the unsaturated soil zone (see Barnes and Allison, 1988), with similar enrichment potential to that observed in leaf water (Barbour, 2007), but also is known to occur to a lesser extent in shallow soils subject to evaporation, or intermittently during evaporation of interception storage. Isotopic discrimination during plant water uptake has also been suggested as a process that can leave a large imprint on finite soil water supplies (Vargas et al., 2017). From the watershed perspective, we acknowledge that a potentially wide range of isotopic signatures may develop within non-mobile soil water storages, which may in some cases directly influence the isotopic composition of transpired moisture or may indirectly affect evaporative enrichment by modifying the isotopic composition of the atmospheric boundary layer in the region. But because non-mobile waters are generally not returned to the stream, they are not significantly affecting the isotopic signals in discharge. Despite being important factors influencing short-term conditions at the hillslope or stand level, we postulate that these storages account for a negligible fraction of the annual runoff volume in most watersheds, and are therefore considered less influential in modifying the isotopic signatures of streamflow, evaporate and transpirate. It remains to be established if TWW might be a more influential control on vapour

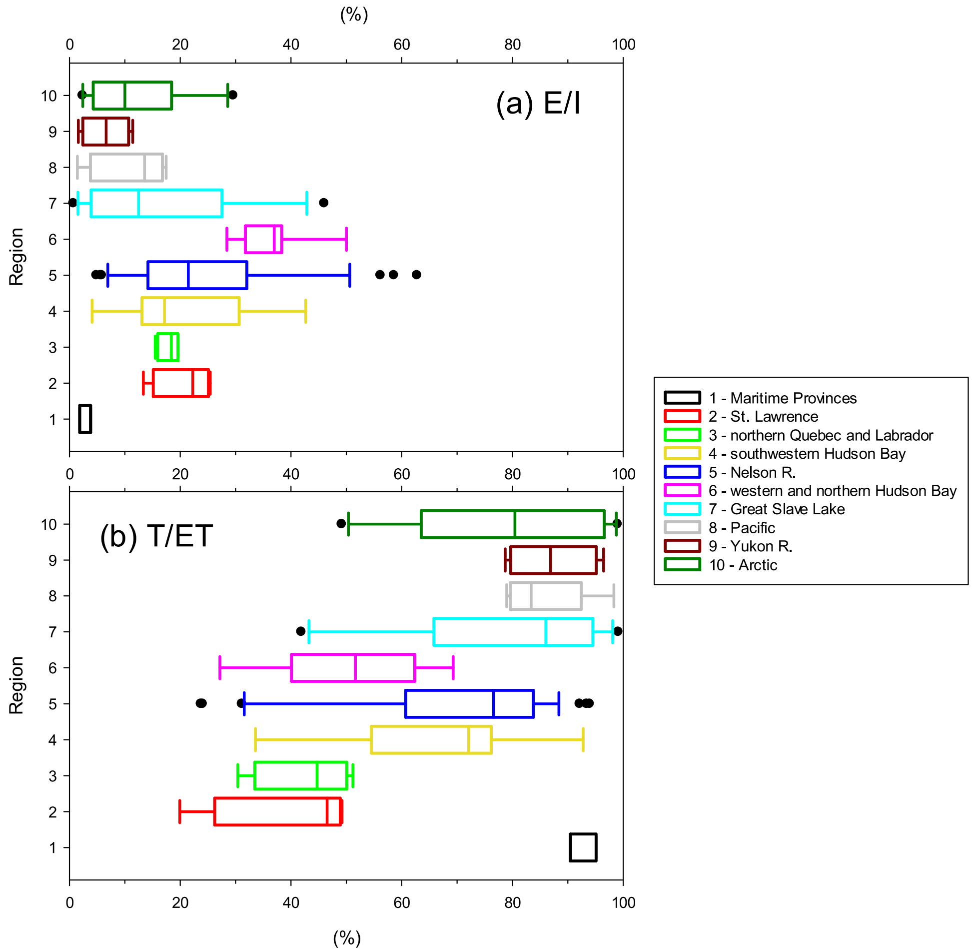

Fig. 3. Box plots summarizing model outputs for watersheds by hydrometric region, comparing: (i) evaporation/inflow and (ii) transpiration/evapotranspiration. Boxes indicate the median and 25th and 75th percentiles, whiskers indicate the 10th and 90th percentiles. Individual outliers are shown.

partitioning in some watersheds if similar approaches were applied in higher frequency time-series sampling programs.

3.2. Evaporation loss and ET partitioning

Evaporation loss (E/I) and transpiration ratios (T/ET) were estimated based on Eqs. (4) and (8), respectively, and are presented by hydrometric region (Fig. 3). Use of long-term climate data and flow-weighted averages was intended to derive values representative of long-term, watershed-integrated fluxes. Comparisons were made for T/ET using the base case model which incorporated interception loss (i.e., Eq. (8)) and a simplified model without interception (i.e., Eq. (9)). While E/I spans a range of values for watersheds within each hydrometric region, systematic differences emerge from region to region, largely reflecting the degree of influence of lakes and wetlands in the drainage network across each region. We note that watersheds within the Maritime Provinces (Region 1) and the Pacific, Yukon and Arctic (Regions 8 through 10) have the lowest E/I ranges varying from 3 to 15 % on average, as compared to Hudson Bay drainages (Regions 4, 5 and 6) that have higher average E/I ratios ranging from 15 to 35 %, and less commonly ranging up to 60 % for individual watersheds. Great Slave Lake drainages (Region 7) are found to have wide-ranging values, with higher E/I values (up to 45 %) for Shield drainages with abundant lakes, as compared to the Peace-Athabasca River basins, which drain both mountainous and low-lying wetland dominated areas and bring the regional average down to approximately 10 %. By comparison, E/I for the Great Lakes/St. Lawrence watersheds, as well as northern Quebec and Labrador are fairly restricted, and in the vicinity of 20 %, reflecting the importance of both small and large lakes in the drainage network.

T/ET is evidently greater than 80 % on average across the Maritime Provinces (Region 1), as well as Great Slave Lake, Pacific, Yukon and Arctic watersheds (Regions 7, 8, 9 10); although the Arctic and Great Slave Lake regions (Regions 10 and 7, respectively) include watersheds with much lower T/ET, ranging down to 40–50 %, due largely to the dominance of lakes and wetland areas, as well as the abundance of non-vegetated outcrop. Transpiration ratios in the Hudson Bay drainages (Regions 4, 5 and 6) range from 50 to 75 %, whereas Great Lakes/St. Lawrence and northern Quebec/Labrador are in the 40–50 % range, apparently controlled mainly by the fraction of lakes and wetlands in these drainage basins.

While these results are a first approximation, given that they can be improved by refining estimates of the flow-weighted isotopic composition of the watersheds, they provide important new information on the dominant vapour loss mechanism, weighted over contributing areas of the watersheds. We note that for watersheds with large partial (or non-) contributing areas, isotope results may not be representative of the entire watershed area, but rather of the relatively smaller area contributing to flow. As noted in previous studies (Fang et al., 2010; Wolfe et al., 2019; Muhammad et al., 2019), non-contributing areas occur widely in the semi-arid, southern prairie watersheds of the Nelson River drainage (Region 5) and in the Milk River (Region 11), the latter of which was not included in this assessment but is part of a transboundary isotopic assessment in progress. Such grassland regions with low, hummocky relief are known to be frequently disconnected from higher order streams (Shook et al., 2015). Other informative examples can be drawn from semi-arid regions such as the Darling River basin in Australia (Gibson et al., 2008b) where the main river channel was shown to be largely disconnected from its upstream contributing area except during storm events, or due to diversion of river water for irrigation of crops. In general, the presence of partial or non-contributing areas is likely to underestimate areal T/ET ratios for the watershed as a whole given that non-connected areas of predominantly grasslands are likely to be dominated by transpiration. Nevertheless, such isotope-based estimates may compliment physically-based water balance assessments, helping to constrain the overall dynamic effect

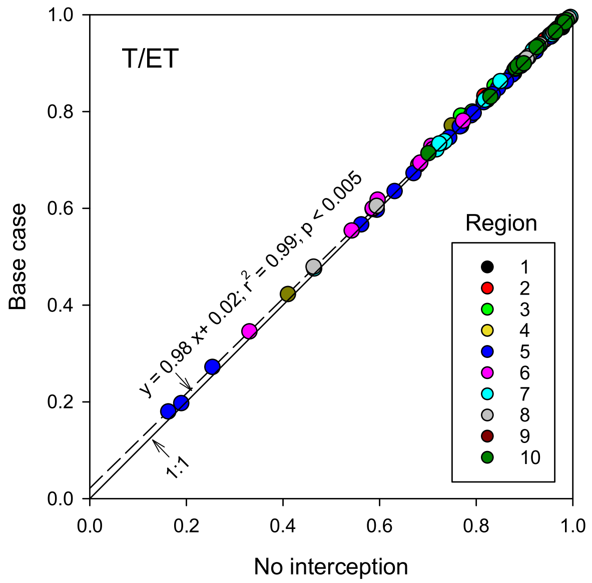

Fig. 4. Crossplot of T/ET based on base case model (Eq. 8) versus no interception model (Eq. 9). Regression line through results is compared to the 1:1 line.

of non-contributing areas in wet and dry years or seasons.

3.3. Effect of interception losses and sublimation on T/ET

Several ET partitioning assessments have included estimates of canopy interception loss under controlled conditions (e.g. Sutanto et al., 2012), although field-based isotopic assessments have commonly encountered difficulties given that isotopic signals due to interception are non-linear, as water is selectively transferred to the soil following evaporation into the atmosphere and associated isotopic exchange that may be partial or complete depending on rainfall frequency, duration and intensity (Allen et al., 2017). To evaluate the importance of interception in determining transpiration ratios, we compare T/ET results from the base case model based on a global, satellite-based reanalysis dataset (GLEAM, Miralles et al., 2010) to a version of the model that neglects interception. To our knowledge, no previous watershed-based isotopic assessments have evaluated the effect of incorporating interception loss. As shown in Fig. 4, we compare T/ET using Eqs. (8) and (9) but find only minor differences between the models, amounting to ±1.6 % difference on average (standard deviation of 5 %). From this we conclude that interception (*N*) likely has a negligible influence on watershed-integrated T/ET estimates for Canada.

While sublimation losses are not explicitly accounted for in this assessment, we recognize that some previous studies have shown sublimation to produce enrichment of the residual snowpack, leading to offset below the meteoric water line (Sokratov and Golubev, 2009). In other cases, no detectable systematic isotopic changes in the residual snowpack due to sublimation were observed (St. Amour et al., 2005).

With regards to our T/ET assessment, sublimation losses would likely result in minor enrichment of streamflow where fractionation is prevalent, a signal which would be incorporated within the non-biotic (evaporative) water loss fraction, and so classified here as an evaporative water loss. As noted by Pang et al. (2019) for sites in East Antarctica, concurrent observations of stable isotopes in atmospheric water vapor, precipitation, and surface snow would be necessary to quantify net changes in the isotopic composition of surface snow due to sublimation.

3.4. Runoff versus vapour loss from watersheds

Watersheds are classified according to dominant water loss mechanisms (Fig. 5). Of the 103 watersheds examined, only 19 had water losses that were runoff-dominated whereas 84 were vapour-dominated. Among vapour-dominated watersheds, 54 were transpiration-dominated and only 5 were evaporation-dominated. A total of 27 watersheds were classified as mixed, having more than one dominant water loss mechanism. Geographically, the transpiration-dominated watersheds are situated largely within western

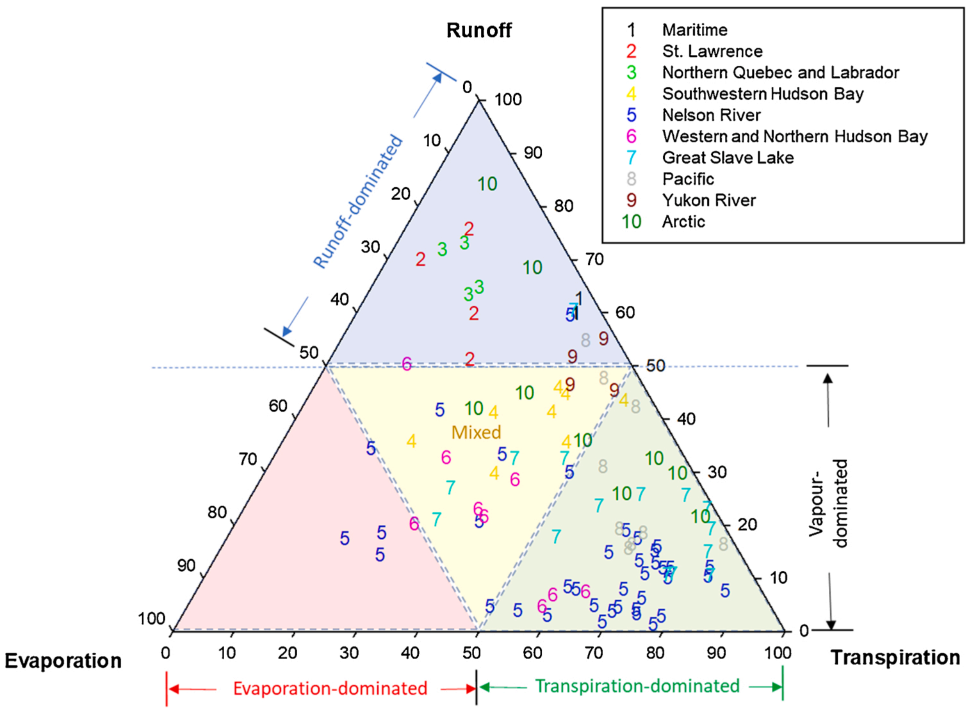

Fig. 5. Ternary classification of watersheds based on percentage of long-term water loss mechanisms (% runoff vs. % evaporation vs. % transpiration). Watersheds are numbered and colour-coded by hydrometric region. Shaded fields indicates evaporation-dominated outflows (red), transpiration-dominated outflow (green), runoff-dominated (blue), mixed or no dominant mechanism (yellow). A colour version of this figure is provided in the web edition.

Canada in Prairie, Boreal Plains, Taiga Plains and Montane ecoregions (Wiken, 1986) within hydrometric Regions 4–8, and 10 (Fig. 6). Runoff-dominated watersheds are widely distributed across eastern Canada (Regions 1–3) as well as within Montane watersheds of western Canada (Regions 5, 8–10). Evaporation-dominated watersheds are the most restricted geographically, being found only in Boreal watersheds, apparently confined to watersheds with a high degree of lake cover near the Boreal/Prairie fringe in Regions 5 and 6. Mixed water-loss watersheds appear to be found most commonly within the Boreal, Taiga, and central Arctic Tundra ecozones including treeline areas of Regions 4–10 (Fig. 6). The Seal River (Region 6), which drains tundra, wetland and forested areas of northern Manitoba and southern Nunavut, is found to be runoff-dominated, which we expect is more typical of watersheds on the western shores of Hudson Bay. It is informative to note that water loss mechanisms appear to evolve from headwaters to mouth within the largest river basins. For example, the 2575-km Nelson River (Region 5), which traverses a wide range in latitude, climatic zones, and physiographic sub- regions, exhibits diverse and evolving water loss mechanisms within its sub-basins. Runoff-dominated tributaries are found in alpine headwaters of Region 5 including the Bow River, Alberta; evaporation-dominated tributaries are found in Precambrian Shield headwaters south of Lake Winnipeg, Manitoba and near Lake of the Woods, Ontario (see inset, Fig. 6); transpiration-dominated tributaries are found for Prairie headwaters; and mixed water loss mechanisms are found for Boreal watersheds, including several rivers such as the Souris River, Mossy River, Limestone River and Odei River, which carry upstream drainage in Region 5 across lake-rich Precambrian Shield terrain to Hudson Bay. For the 4241-km Mackenzie River system, a similar evolution of dominant water loss mechanisms from headwaters to mouth is noted. Rocky Mountains headwaters of the Athabasca River are runoff-dominated where monitored at Hinton, Alberta, whereas Precambrian Shield headwaters are mixed, and wetland-dominated watersheds along the Peace-Athabasca-Mackenzie corridor are transpiration-dominated. In the following section we further explore water balance variations in watersheds across Canada through more detailed analysis of land cover controls.

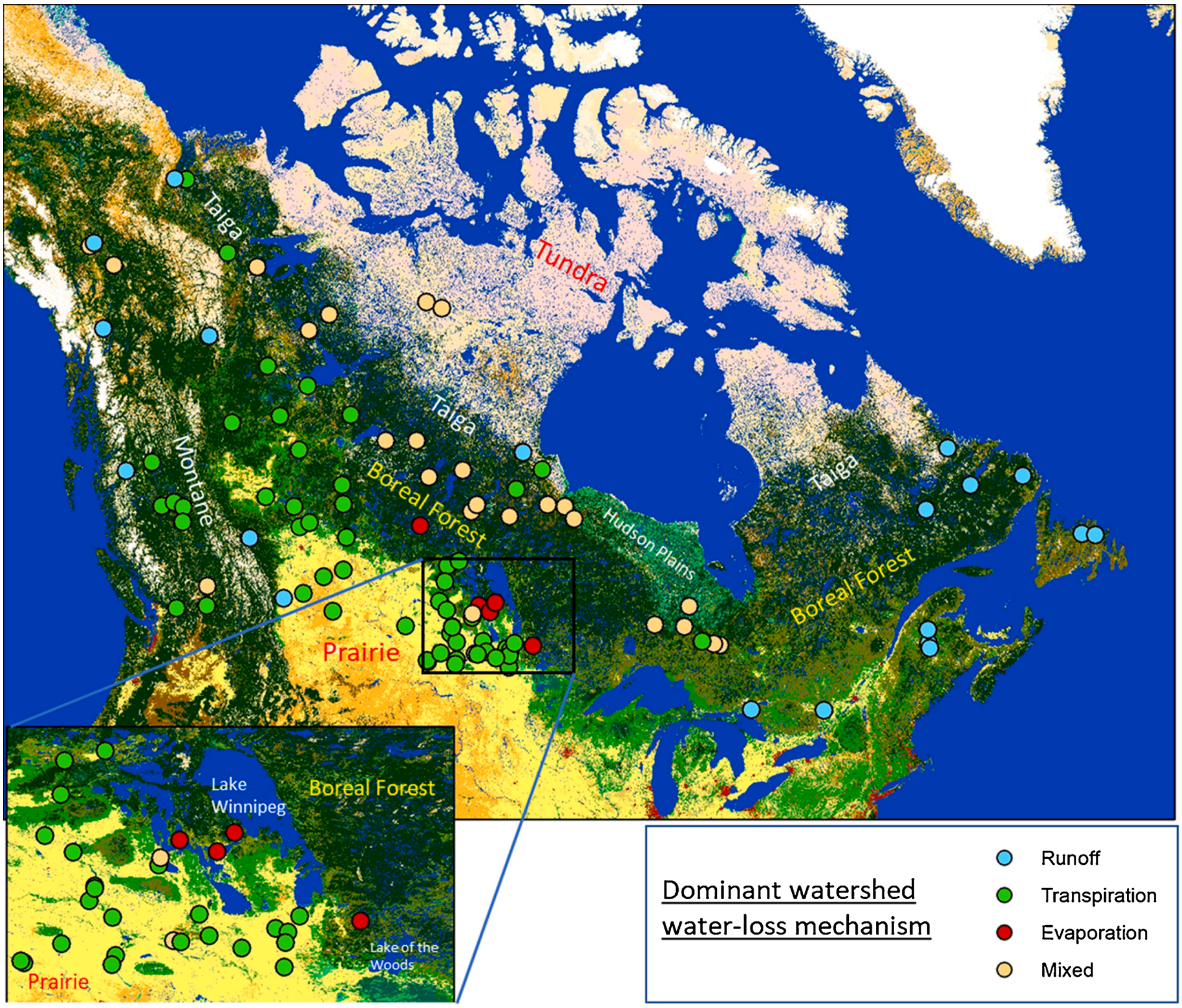

Fig. 6. Map showing dominant water-loss mechanisms for study watersheds as classified by isotope-based analysis, overlain on CCI-LS land cover distribution (www.esa-landcover-cci.org). Inset shows enlargement of southern Manitoba region. Legend is provided online (maps.elie.ucl.ac.be/CCI/viewer/download/CCI-LC_Maps_Legend.pdf).

(a) Transpiration/Evapotranspiration

WSC region	CCI-LC Description	Cropland	Forest cover	Selected forest subtypes				Shrubland/ Grassland	Lichen/ Moss	Sparse shrub	Wetlands	Open water	Open water + wetland
				Needleleaf, Evergreen, Closed	Needleleaf, Evergreen, Open	Total Deciduous	Mixed leaf						
		10,20	50, 60, 70, 80, 90	71	72	60,80	90	120,130	140	152	160, 170,180	210	160, 170, 180, 210
1	Maritime	-0.020	0.093	**-0.347**	**-0.276**	**0.472**	0.242	**-0.372**	-0.165	-0.036	-0.182	-0.110	-0.094
2	St. Lawrence	--	-0.738	-0.738	--	-0.738	-0.738	-0.738	-0.258	--	-0.738	-0.949	-0.949
3	n. Quebec Labr.	--	0.000	0.800	-1.000	0.200	0.000	-0.800	-0.400	-0.105	0.000	0.600	0.600
4	sw Hudson Bay	--	0.395	**-0.778**	**-0.764**	-0.371	0.395	**-0.755**	**-0.748**	0.412	**-0.802**	**-0.778**	**-0.802**
5	Nelson R.	**0.403**	-0.213	-0.031	0.002	0.002	-0.273	0.089	-0.081	0.217	-0.204	**-0.461**	**-0.458**
6	w/n Hudson Bay	0.627	0.217	-0.233	-0.209	0.483	0.333	-0.250	-0.333	--	0.017	**-0.800**	-0.383
7	Great Slave Lake	0.262	-0.414	0.354	-0.013	0.450	**0.614**	0.250	-0.439	**0.651**	0.304	**-0.732**	**-0.818**
8	Pacific	0.502	**0.667**	-0.433	0.285	0.333	-0.033	0.567	-0.250	0.434	0.500	-0.517	-0.517
9	Yukon R.	--	0.600	0.000	0.600	-0.400	-0.400	0.000	-0.600	0.000	0.800	-0.400	-0.400
10	Arctic	0.450	0.552	**0.624**	-0.043	**0.644**	0.515	0.164	-0.146	-0.089	**0.648**	-0.055	0.176

(b) Evaporation/Inflow

WSC region	CCI-LC Description	Cropland	Forest cover	Selected forest subtypes				Shrubland/ Grassland	Lichen/ Moss	Sparse shrub	Wetlands	Open water	Open water + wetland
				Needleleaf, Evergreen, Closed	Needleleaf, Evergreen, Open	Total Deciduous	Mixed leaf						
		10,20	50, 60, 70, 80, 90	71	72	60,80	90	120,130	140	152	160, 170,180	210	160, 170, 180, 210
1	Maritime	0.127	-0.172	0.054	0.048	-0.157	**-0.346**	0.168	0.057	-0.175	-0.134	0.198	0.135
2	St. Lawrence	--	-0.632	-0.632	--	-0.632	-0.632	-0.632	-0.775	--	-0.632	-0.211	-0.211
3	n. Quebec Labr.	--	0.800	-0.800	0.400	-0.800	-0.800	-0.200	1.000	-0.632	-0.800	0.400	0.400
4	sw Hudson Bay	--	-0.503	**0.695**	**0.764**	0.311	-0.503	0.671	**0.748**	-0.412	**0.719**	**0.695**	**0.719**
5	Nelson R.	**-0.295**	0.077	-0.025	-0.006	-0.033	0.168	-0.046	0.050	-0.217	0.150	**0.411**	**0.408**
6	w/n Hudson Bay	-0.287	-0.433	0.450	0.000	-0.133	0.150	-0.067	-0.150	--	0.483	0.617	**0.883**
7	Great Slave Lake	-0.234	0.461	-0.364	-0.079	-0.364	**-0.532**	-0.314	0.386	**-0.580**	-0.218	**0.714**	**0.836**
8	Pacific	-0.388	-0.617	0.267	-0.259	-0.250	-0.050	-0.417	0.383	-0.525	-0.600	**0.667**	**0.667**
9	Yukon R.	--	-0.600	0.000	-0.600	0.400	0.400	0.000	0.600	0.000	-0.800	0.400	0.400
10	Arctic	**-0.623**	-0.248	-0.576	-0.399	-0.480	**-0.927**	-0.261	0.109	-0.539	-0.382	0.127	-0.067

Legend
-1
-0.8
-0.6
-0.4
-0.2
0
0.2
0.4
0.6
0.8
1
p < 0.05
p >0.05

Fig. 7. Heatmap diagram illustrating Spearman rank order correlations between isotope-based indicator values and landcover classes stratified by hydrometric region. Colours indicate correlation strength and direction; bold entries indicate significant correlations ($p < 0.05$) (see Legend). Note that hybrid land classes (e.g. cropland) are used based on grouped CCI-LC land classes (numbered 10 to 210), as provided in Table S1.

3.5. Land cover effects

Land cover characteristics for the studied watersheds was obtained from CCI-LS (ESA, 2017), which differentiates 22 land cover classes globally based on the United Nations Land Cover Classification System (LCCS) (Di Gregorio and Jansen, 2000). To eliminate classes that were absent or unimportant in North America, to highlight land cover characteristics considered to be influential for determining T/ET, E/I, and for classification of dominant water losses, a simplified set of 12 land classes was used, some comprised of amalgamated CCI-LS classes (Fig. 7, Table S1). As transpiration is linked to photosynthesis in vascular plants whereas evaporation is linked to abiotic vapour losses (i.e. mainly open water evaporation), we hypothesize that greater percent forest cover, grassland and cropland cover is likely to be associated with enhanced T/ET, whereas surface water storage (e.g. lakes and wetlands) is likely to be associated with enhanced E/I. A heatmap diagram provides a test of these hypotheses (Fig. 7).

We find that T/ET is positively correlated with cropland in watersheds having extensive cultivation (e.g. Region 5), and positively correlated with forest cover in general, although strength of the correlation among the various forest types depends on their importance within each region. For example, correlation between T/ET and deciduous forest is more robust for the Maritimes (Region 1), whereas correlation between T/ET and needleleaf evergreen is more robust in boreal/arctic regions of northern Quebec and Labrador, Great Slave Lake, and the Arctic (Regions 3, 7, and 10).

T/ET appears to be insensitive to percent shrubland and grassland, presumably because these areas tend to be dominated by open water. As expected, E/I is positively correlated with open water in all regions except the St. Lawrence, which is fed by evaporatively enriched water from the Great Lakes system (see Jasechko et al., 2014b; Karim et al., 2008). For this reason, isotopic enrichment and indicators such as E/I are not a sensitive cumulative indicator of evaporation losses for the lower St. Lawrence watershed, which was predicted for such basins by Gat's (2010) river continuum model. E/I is positively correlated with the following land cover types: (i) wetland cover in the Hudson Bay drainages (Regions 4, 5, and 6), (ii) lichen/moss cover in regions where it is abundant (across most of northern Canada; Regions 1,3–5, 7–10), and (iii) open/closed needleleaf evergreen in southwestern Hudson Bay (Region 4). Note that lichen and mosses are non-vascular, and therefore respiration is accomplished by evaporation rather than transpiration (Price et al., 2009). Therefore, lichen/moss land cover is positively correlated with E/I and negatively correlated with T/ET.

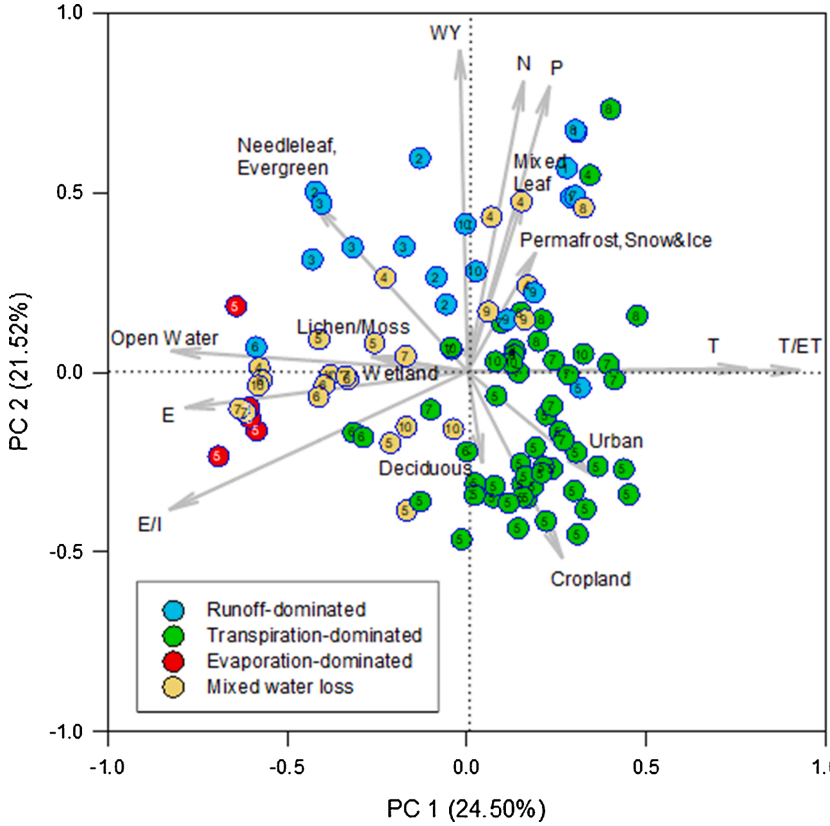

Fig. 8. PCA biplot illustrating scores for individual watersheds (points) overlain by loadings (vectors) based on land cover characteristics. Principal components explain 24.50 % (PC1) and 21.52 % (PC2) of variability within the dataset. Points are differentiated by dominant water loss mechanism, with number labels indicating hydrometric regions. Variations along PC1 are controlled mainly by transpiration-dominated versus evaporation-dominated water losses, whereas variations on PC2 mainly reflect runoff-dominated versus mixed or vapour-dominated water losses. See text for further discussion.

Overall, our general hypothesis that open water and wetlands were the dominant drivers of E/I is verified, and to some extent the inverse is found to be true for T/ET, where watersheds with reduced wetland and open water generally had higher T/ET. Direct correlation between T/ET and various forest cover types is, however, found to be region-specific and less systematic; although patterns appear to be more predictable when both vapour and liquid water losses are considered together. While we expected to detect the influence of cropland development on E/I and T/ET in agricultural areas, we were not anticipating that this effect would be quite as pronounced. Most notably, the significant correlations between cropland cover and T/ET for the Nelson R. basin (Region 5) indicates that watershed management decisions may have a pronounced impact on the vapour partitioning mechanisms.

To further explore the effect of land cover on the dominant water loss mechanisms in watersheds across Canada, we applied principal components analysis (PCA) to offer additional insight into vegetation drivers of vapour loss and runoff. Analogous methods have been applied to examine hydroclimatic controls on runoff (Gibson et al., 2015, 2019) and trophic status (Gibson et al., 2016c). As shown in a PCA biplot (Fig. 8), watersheds with similar vegetation characteristics cluster together, with scores close to the origin reflecting near-average characteristics, and scores offset from the origin reflecting degree of departure from average characteristics attributable to variable loadings (vectors). Note that subparallel loading vectors are highly correlated, whereas correlation decreases in direct proportion to angle of offset between vectors, culminating in perpendicularity for uncorrelated factors. This allows for comparison between water balance characteristics and vegetation characteristics across the entire dataset.

Notably, we find the following: (i) a negative correlation between E or E/I versus T or T/ET, (ii) lack of correlation between water yield (WY) and E, E/I, T, E/T, (iii) strong correlation between WY, N and P, (iv) runoff-dominated watersheds are most often needleleaf evergreen, but less commonly may be mixed leaf forest, or contain significant areas of permanent snow and ice (v) P and N tend to be higher for mixed leaf forests, (vi) transpiration-dominated watersheds are most commonly cropland, with secondary influences being deciduous forest and urban areas, and (vii) mixed water loss and evaporation-dominated water loss in watersheds are commonly associated with open water, lichen and moss, and wetlands. While further work is warranted on a watershed by watershed basis to evaluate the specific effects of C3 versus C4 plant cover, runoff organization, elevation, surface roughness, groundwater-surface water interactions, and permafrost conditions, our first approximation analysis suggests that basic land cover characteristics exert significant influence on the partitioning results. Time-series analysis based on long-term water sampling and isotope partitioning may therefore be informative for examining both climatic and land use impacts on the hydrological cycle.

3.6. Towards improved understanding of water and carbon cycle interactions

Previous watershed studies have applied isotope-based water balance results to estimate important carbon cycle indicators, including net primary productivity (Lee and Veizer, 2003). Because transpiration alone is linked to photosynthesis, the T/ET ratio and estimates of water use efficiency can be used to estimate net primary productivity of each watershed. This is a potentially powerful tool for tracking impacts of land use and climate change on both the water and carbon cycles, especially considering that it provides areal estimates that are representative of the watershed and are cumulative due to flow-weighting. As noted by Gibson et al. (2005), watershed-based ET partitioning using isotopes offers a complimentary perspective to tower-based flux monitoring methods and may offer an additional opportunity to track changes on a watershed scale.

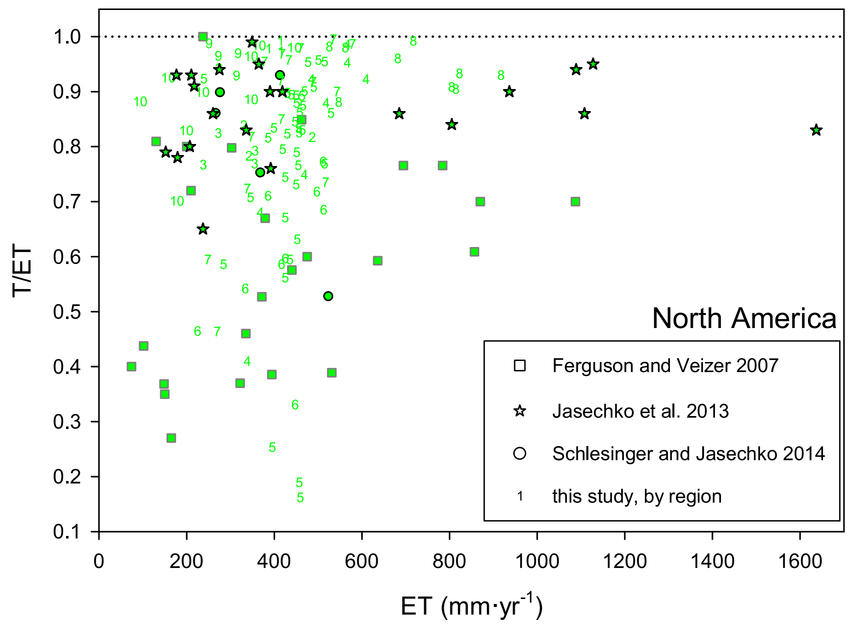

Fig. 9. Crossplot comparing total evapotranspiration flux and proportion that occurs by transpiration for North American watersheds according to previous investigations and this study.

3.7. Comparison with continental and global studies

We compared the results of our watershed ET assessments across Canada presented here with previous studies reported for river basins in North America and globally, including those of Jasechko et al. (2013), Schleisinger and Jasechko (2014) and Ferguson and Veizer (2007). For North America (Fig. 9), we found reasonable consistency overall for determinations of T/ET, although our dataset lacked examples of temperate forests provided by Ferguson and Veizer (2007) that were characterized by high ET and mid-range T/ET values (i.e. 60–80 %), and also lacked examples from the Laurentian Great Lakes and central inland seas (Tahoe, Nicaragua) presented by Jasechko et al. (2013) that had high ET (700–1600 mm/yr) and T/ET ratios in the 85–95 % range. Our analysis contained more examples of high latitude watersheds with both high T/ET (mostly western and northern Canada) and low T/ET (from the lake and wetland-rich Nelson R. basin). Average values of T/ET (±std) for our watersheds was 80.3 ± 20.7 % which was similar to isotope-based estimates of Ferguson and Veizer for North American river basins (79.4 ± 16.3 %), but lower than isotope-based estimates of T/ET for large lake watersheds (87.8 ± 8.0 %) presented by Jasechko et al. (2013). Some of these differences may be attributed to catchment-scale processes, as argued by Schlaepfer et al. (2014), who contended that lakes may not be ideal reservoirs for capturing terrestrial ecosystem signals. This is likely the case for arid or seasonally arid watersheds that may only be partially connected or periodically connected to the surrounding watershed. Schleisinger and Jasechko (2014) described this effect as "hydrologic decoupling" which was invoked to explain lower T/ET values based on field-based stand-level monitoring methods (e.g. sap or radial flow measurements, diurnal water table monitoring, energy balance, eddy co-variance, aerodynamic profiling, isotopic flux tracing). For North American watersheds. Schleisinger and Jasechko (2014) estimated average T/ET at 59.7 ± 19.4 %, but acknowledged that poor characterization of subcanopy transpiration, limited duration of stand-level measurements that often do not extend to include the entire growing season, and difficulty in extrapolating to the watershed scale, may contribute to this differential.

3.8. Uncertainty in estimation of E/I and T/ET

Uncertainty in estimation of E/I for river watersheds using similar methodology to that presented here was reported to be 12–17 % for 4 large watersheds in North America (Ferguson and Veizer, 2007), and this is shown to be the principal uncertainty carried through in the isotope-based calculation of T/ET. As revealed by the sensitivity analysis presented by Gibson et al. (1993), in a Monte Carlo uncertainty analysis by Jasechko et al. (2013), and also displayed in the uncertainty estimates of Ferguson and Veizer (2007), non-linearity of the evaporative isotopic enrichment produces higher uncertainty for near-terminal systems, i.e. E/I (%) is close to 100 %, and also for systems with low evaporation losses. As a consequence, uncertainty in the range of 35–96 % is reported by Ferguson and Veizer (2007) for several African River basins that apparently approach terminal status, and uncertainty of 40 % is estimated for the Mississippi River, which does not significantly deviate from the meteoric water line (Lee and Veizer, 2003). Likewise, uncertainties are estimated at 28 % and 17 %, respectively for the Murray-Darling River basin, Australia (E/I∼22 %) and two humid Oceania watersheds (E/I∼6 %) (Ferguson and Veizer, 2007).

As a test of the reproducibility of the results for specific watersheds in Canada, we compared our results with the estimates of Telmer and Veizer (2000) for the Ottawa River basin and Ferguson et al. (2007) for the Saskatchewan River basin, and found these to be in agreement with our estimates to with 7 % and 3 % respectively, despite being based on different periods of record for climate, discharge, and isotopic composition of streamflow. This finding also lends support for our defined limits of uncertainty.

3.9. Implications for improved models and hydrometric prediction

The isotope partitioning approach presented here allows for field-based quantification of evaporation and transpiration partitioning, which offers an independent approach for evaluating and/or validating model-based estimation or parameterization of these vapour fluxes. This is particularly useful for long-term water balance studies where the correct apportionment of water loss and storage within hydrologic models directly impacts estimation of future runoff and discharge. Such estimates can be particularly sensitive in inflow-limited environments, such as across the Canadian Prairies, which leads to considerable uncertainty in the estimation of future runoff (Stadnyk et al., 2019).

Process-based apportionment of water within hydrologic models has been shown to be complex and subject to equifinality, or many possible solutions all resulting in the same statistical outcome, when evaluated against discharge alone (Beven and Freer, 2001). The inclusion of isotope tracers in hydrologic model calibration can, however, better inform the model calibration and process-based partitioning within hydrologic models (Stadnyk and Holmes, 2020; Holmes et al., 2020). Holmes et al. (2020) demonstrated that statistically equivalent model performance could be obtained by very different internal water balance structures, or process-based partitions. The difficulty was in evaluating the correctness of the various partitions due to a lack of regional evaporation and transpiration-based partitions at the scale the model was developed. The methods demonstrated in this study are appropriate to independently estimate evaporation and transpiration-based loss at the watershed scale, providing an independent and scale-appropriate dataset for model evaluation.

These methods are particularly useful in regions where hydrometric data do not exist (ungauged basins), but where there are existing isotope data and/or the capability to collect isotope data. Our methods therefore extend to predictions in ungauged basins by offering a means to estimate evaporation and transpiration losses in ungauged basins. Similarly, we can extend the application of our methodology to future predictions using isotope-enabled climate and hydrologic models. The prediction accuracy of such models is focused (through calibration and evaluation of hindcast scenarios) on precipitation amount and temperature. Secondary variables, such as evaporation loss and discharge, are projected but with considerable uncertainty. This methodology provides a means of improving future projections by constraining potential uncertainties in future projections at regional or continental scales.

On the topic of uncertainty, there exists the potential to directly assess the uncertainty associated with non-stationarity in land cover/land use through time by correlating a watershed primary water balance control to landcover transitions or states. By deriving a connection between landcover and water yield, or the primary runoff generating mechanism (e.g., Fig. 8), we can quantify the influence landcover change has on runoff generation without directly measuring changes in individual water balance components. This offers significant opportunity for watershed management and sustainable land use planning.

3.10. Benefits and limitations

Application of isotope-based partitioning in conjunction with routine hydrometric monitoring, as demonstrated here, provides an integrated approach for characterization of both runoff and vapour loss mechanisms at the regional or watershed scale, and thereby establishes a more complete perspective on water cycling dynamics, as well as capturing an important indicator of carbon cycling via the linkage between transpiration fluxes and photosynthesis. One principal benefit of long-term monitoring of isotope signals in rivers is that it offers a practical method for monitoring watershed scale changes, and perhaps may even serve as an early warning indicator of hydrologic change and susceptibility related to climate and land cover alteration.

One of the primary limitations of the current dataset is that it is of restricted duration and scope and is spatially inconsistent, therefore flow-weighted averages are approximate as they were accrued from non-uniform interannual sampling, rather than being based on identical sampling schedules at all gauging stations. Fortunately, additional and consistent sampling in the future across an identified network of stations will only improve flow-weighted averages. A more significant limitation in use of isotopes in time-series monitoring mode is that it will require re-activation and improvement of the Canadian Network for Isotopes in Precipitation (CNIP), which has operated periodically over the past several decades (see Birks and Gibson, 2009). Better understanding of the role of pre-modern water sources including permafrost thaw, glacial meltwater, and glaciogenic groundwater sources, and consideration of changes in watershed storage in general may require more sophisticated distributed models, which are readily available.

4. Summary and conclusions

Canada-wide water sampling for stable isotopes (^{18}O and ^{2}H) was conducted at selected Water Survey gauging stations, providing the first comprehensive national streamflow dataset. 331 watersheds across 10 hydrometric regions, ranging in size from 10 to 10,000 km^2, were monitored. 161 gauging stations had sufficient sampling to estimate flow-weighted discharges, and 103 watersheds were selected for vapour partitioning analysis.

Based on the Craig and Gordon (1965) model, a watershed-based method for vapour partitioning is developed and applied in 103 watersheds. Variations in these vapour partitioning indicators reveal systematic responses across a range of land cover types and climate zones, spanning over 25° latitude and 86° longitude. The method compares favorably with previous applications of isotopic partitioning methods at the watershed scale (e.g. Ferguson and Veizer, 2007; Jasechko et al., 2013) and may provide practical context for comparing and extending vapour partitioning studies and water-carbon cycle interaction studies from stand-level to the continental scale.

Important water cycle indicators were derived at the watershed scale including evaporation/inflow (E/I) and transpiration/evapotranspiration (T/ET). E/I is found to be controlled mainly by open water and wetland extent, whereas T/ET is controlled by forest cover and cropland extent. Calculations suggest that E/I ranged from 2 to 60 % and T/ET ranged from 25 to 95 % across a wide range of watersheds. Sensitivity analysis suggests only a minor influence on vapour partitioning at the watershed scale related to interception.

A new water loss classification approach is introduced which reveals that 19 of 103 watersheds were runoff-dominated, 54 were transpiration-dominated, 5 were evaporation-dominated, and 27 had more than one dominant water loss mechanism.

Planned future studies include ongoing monitoring of the streamflow network, comparison with simulations from a range of distributed hydrological models, and further analysis of streamflow sources using hydrograph separation methods as well as various other frequency analysis techniques (see Jasechko et al., 2016) that will enable further insight into the age and sources of streamflow.

CRediT authorship contribution statement

J.J. Gibson: Conceptualization, Data Curation, Methodology, Formal Analysis, Validation, Visualization, Writing, Editing, Project Administration, Funding Acquisition. **T. Holmes:** Spatial Analysis, Coding, Visualization, Formal Analysis, Review. **T.A. Stadnyk:** Conceptualization, Writing, Editing, Review. **S.J. Birks:** Conceptualization, Review. **P. Eby:** Laboratory Analysis. **A. Pietroniro:** Conceptualization, Project Administration, Field Coordination, Funding Acquisition, Review.

Declaration of Competing Interest

The authors report no declaration of interest.

Acknowledgements

Funding and in-kind support for analytical costs and logistics was provided by Environment and Climate Change Canada via Grants and Contributions Agreements and by InnoTech Alberta via Internal Investment Grants. We sincerely thank the staff of Water Survey of

Canada for their skilled support for water collection, labelling and shipping, and for knowledge of the regional hydrology which assisted with sampling and troubleshooting issues in the field. We gratefully acknowledge Jenna Merth, University of Calgary, for providing Matlab and GIS support.

Appendix A. Supplementary data

Supplementary material related to this article can be found, in the online version, at doi:https://doi.org/10.1016/j.ejrh.2021.100878.

References

Ala-aho, P., Soulsby, C., Pokrovsky, O.S., Kirpotin, S.N., Karlsson, J., Serikova, S., Manasypov, R., Lim, A., Krickov, I., Kolesnichenko, L.G., 2018. Permafrost and lakes control river isotope composition across a boreal Arctic transect in the Western Siberian lowlands. Environ. Res. Lett. 13 (2008), 034028 https://doi.org/10.1088/1748-9326/aaa4fe.

Allen, S., Keim, R.F., Barnard, H.R., McDonnell, J.J., Brooks, J.R., 2017. The role of stable isotopes in understanding rainfall interception processes: a review. WIREs Water 4, e1187. https://doi.org/10.1002/wat2.1187, 2017.

Allison, G.B., Barnes, C.J., Hughes, M.W., 1983. Distribution of deuterium and oxygen-18 in dry soils: II experimental. J. Hydrol. 64, 377–397.

Barbour, M.M., 2007. Stable oxygen isotope composition of plant tissue: a review. Funct. Plant Biol. 83–94, 2007.

Barnes, C.J., Allison, G.B., 1988. Tracing of water movement in the unsaturated zone using stable isotope of hydrogen and oxygen. J. Hydrol. 100, 143–176.

Belachew, D.L., Leavesley, G., David, O., Patterson, D., Aggarwal, P., Araguas, L., Terzer, S., Carlson, J., 2016. IAEA Isotope-enabled coupled catchment-lake water balance model, IWBMIso: description and validation. Isotopes Environ. Health Stud. 4-5, 427–442.

Berg, A., Sheffield, J., 2019. Evapotranspiration partitioning in CMIP5 models: uncertainties and future projections. J. Climate 32, 2653–2671.

Beven, K., Freer, J., 2001. Equifinality, data assimilation, and uncertainty estimation in mechanistic modelling of complex environmental systems using the GLUE methodology. J. Hydrol. 249, 11–29.

Birks, S.J., Gibson, J.J., 2009. Isotope hydrology research in Canada, 2003-2007. Can. Water Resour. J. 34 (2), 163–176.

Brand, W.A., Avak, H., Seedorf, R., Hofmann, D., Conrad, T.H., 1996. New methods for fully automated isotope ratio determination from hydrogen at the natural abundance level. Isotopes Environ. Health Stud. 32, 263–273.

Coenders-Gerrits, A.M.J., van der Ent, R.J., Bogaard, T.A., Wang-Erlandsson, L., Hrachowitz, M., Savenije, H.H.G., 2014. Uncertainties in transpiration estimates. Nature 506 (7487), E1–E2. https://doi.org/10.1038/nature12925.

Craig, H., Gordon, L.I., 1965. Deuterium and oxygen-18 in the ocean and marine atmosphere. In: Tongiorgi, E. (Ed.), Stable Isotopes in Oceanographic Studies and Paleotemperatures, pp. 9–130. Spoleto, Italy.

Delavau, C., Chun, K.P., Stadnyk, T., Birks, S.J., Welker, J.M., 2015. North American precipitation isotope (δ18O) zones revealed in time series modeling across Canada and northern United States. Water Resour. Res. 51, 1284–1299.

Di Gregorio, A., Jansen, L.J.M., 2000. Environment and Natural Resources Service, GCP/RAF/287/ITA Africover - East Africa Project and Soil Resources, Management and Conservation Service, 179 pages, 28 figures, 3 tables and including CD-ROM. FAO, Rome.

ESA (European Space Agency), 2017. Land Cover CCI Product User Guide Version 2. Tech. Rep.. Available at: maps.elie.ucl.ac.be/CCI/viewer/download/ESACCI-LC-Ph2-PUGv2_2.0.pdf.

Evaristo, J., Jasechko, S., McDonnell, J.J., 2015. Global separation of plant transpiration from groundwater and streamflow. Nature 525, 91–94.

Fang, X., Pomeroy, J.W., Westbrook, C.J., Guo, X., Minke, A.G., Brown, T., 2010. Prediction of snowmelt derived streamflow in a wetland dominated prairie basin. Hydrol. Earth Syst. Sci. Discuss. 892 (14), 991–1006. https://doi.org/10.5194/hess-14-991-2010.

Fekete, B., Gibson, J.J., Aggarwal, P., Vorosmarty, C., 2006. Application of isotope tracers in continental scale hydrological modeling. J. Hydrol. 330, 444–456. https://doi.org/10.1016/j.jhydrol.2006.04.029.

Ferguson, P.R., Veizer, J., 2007. The coupling of water and carbon fluxes via the terrestrial biosphere and its significance to the Earth's climate system. J. Geophys. Res. - Atmos. 112 https://doi.org/10.1029/2007JD008431. D24S06.

Ferguson, P.R., Weinrauch, N., Wassenaar, L.I., Mayer, B., Veizer, J., 2007. Isotopic constraints on water, carbon, and heat fluxes from the northern Great Plains region of North America. Global Biogeochem. Cycles 21, GB2023. https://doi.org/10.1029/2006GB002702, 2007.

Gat, J.R., 2010. Isotope hydrology: a study of the water cycle. In: Series on Environmental Science and Management, vol. 6. Imperial College Press, London, p. 83.

Gibson, J.J., 2001. Forest-tundra water balance signals traced by isotopic enrichment in lakes. J. Hydrol. 251, 1–13.

Gibson, J.J., Edwards, T.W.D., 2002. Regional surface water balance and evaporation-transpiration partitioning from a stable isotope survey of lakes in northern Canada. Global Biogeochem. Cycles 16 (2). https://doi.org/10.1029/2001GB001839.

Gibson, J.J., Reid, B., 2010. Stable isotope fingerprint of open-water evaporation losses and effective drainage area fluctuations in a subarctic Shield watershed. J. Hydrol. 381, 142–150. https://doi.org/10.1016/j.jhydrol.2009.11.036.

Gibson, J.J., Reid, R., 2014. Water balance along a chain of tundra lakes. J. Hydrol. 519, 2148–2164. https://doi.org/10.1016/j.jhydrol.2014.10.011.

Gibson, J.J., Edwards, T.W.D., Bursey, G.G., Prowse, T.D., 1993. Estimating evaporation using stable isotopes: quantitative results and sensitivity analysis for two catchments in northern Canada. Nord. Hydrol. 24, 79–94.

Gibson, J.J., Aggarwal, P., Hogan, J., Kendall, C., Martinelli, L.A., Stichler, W., Rank, D., Goni, I., Choudhry, M., Gat, J., Bhattacharya, S., Sugimoto, A., Fekete, B., Pietroniro, A., Maurer, T., Panarello, H., Stone, D., Seyler, P., Maurice-Bourgoin, L., Herczeg, A., 2002a. Isotope studies in large river basins: a new global research focus. EOS 83 (52), 613–617.

Gibson, J.J., Prepas, E.E., McEachern, P., 2002b. Quantitative comparison of lake throughflow, residency, and catchment runoff using stable isotopes: modelling and results from a survey of boreal lakes. J. Hydrol. 262, 128–144. https://doi.org/10.1016/S0022-1694(02)00022-7.

Gibson, J.J., Edwards, T.W.D., Birks, S.J., St. Amour, N.A., Buhay, W., McEachern, P., Wolfe, B.B., Peters, D.L., 2005. Progress in isotope tracer hydrology in Canada. Hydrol. Process. 19, 303–327.

Gibson, J.J., Sadek, M.A., Stone, D.J.M., Hughes, C., Hankin, S., Cendon, D.I., Hollins, S.E., 2008a. Evaporative isotopic enrichment as a constraint on reach water balance along a dryland river. Isotopes Environ. Health Stud. 44, 83–98. https://doi.org/10.1080/10256010801887489.

Gibson, J.J., Birks, S.J., Edwards, T.W.D., 2008b. Global prediction of δ_A and δ^2H-δ^{18}O evaporation slopes for lakes and soil water accounting for seasonality. Global Biogeochem. Cycles. https://doi.org/10.1029/2007GB002997.

Gibson, J.J., Birks, S.J., Jeffries, D.S., Kumar, S., Scott, K.A., Aherne, J., Shaw, P., 2010. Site-specific estimates of water yield applied in regional acid sensitivity surveys in western Canada. J. Limnol. 69 (Suppl. 1), 67–76. https://doi.org/10.4081/jlimnol.2010.s1.67.

Gibson, J.J., Birks, S.J., Yi, Y., Vitt, D., 2015. Runoff to boreal lakes linked to land cover, watershed morphology and permafrost melt: a 9-year isotope mass balance assessment. Hydrol. Process. 29, 3848–3861. https://doi.org/10.1002/hyp.10502.

Gibson, J.J., Yi, Y., Birks, S.J., 2016a. Isotope-based partitioning of streamflow in the oil sands region, northern Alberta: towards a monitoring strategy for assessing flow sources and water quality controls. J. Hydrol. Reg. Stud. 5, 131–148. https://doi.org/10.1016/j.ejrh.2015.12.062.

Gibson, J.J., Birks, S.J., Yi, Y., 2016b. Stable isotope mass balance of lakes: a contemporary perspective. Quat. Sci. Rev. 131 (B), 316–328. https://doi.org/10.1016/j.quascirev.2015.04.013.

Gibson, J.J., Birks, S.J., Yi, Y., Moncur, M.C., McEachern, P.M., 2016c. Stable isotope mass balance of fifty lakes in central Alberta: assessing the role of water balance and climate in determining trophic status and lake level. J. Hydrol. Reg. Stud. 6, 13–25. https://doi.org/10.1016/j.ejrh.2016.01.034.

Gibson, J.J., Birks, S.J., Jeffries, D., Yi, Y., 2017. Regional trends in evaporation loss and water yield based on isotope mass balance of lakes: the Ontario Precambrian Shield surveys. J. Hydrol. 544, 500–510. https://doi.org/10.1016/j.jhydrol.2016.11.016.

Gibson, J.J., Birks, S.J., Yi, Y., Shaw, P., Moncur, M.C., 2018. Isotopic and geochemical surveys of lakes in coastal British Columbia: insights into regional water balance and water quality controls. J. Hydrol. Reg. Stud. https://doi.org/10.1016/j.ejrh.2018.04.006.

Gibson, J.J., Birks, S.J., Moncur, M.C., 2019. Mapping water yield distribution across the southern Athabasca Oil Sands area: baseline surveys applying isotope mass balance of lakes. J. Hydrol. Reg. Stud. 21, 1–13. https://doi.org/10.1016/j.ejrh.2018.11.001.

Gibson, J.J., Holmes, T., Stadnyk, T., Birks, S.J., Eby, P., Pietroniro, A., 2020. ^{18}O and ^{2}H in streamflow across Canada. J. Hydrol. Reg. Stud. 32, 100754 https://doi.org/10.1016/j.ejrh.2020.100754 (2020) [PDF].

Gibson, J.J., Eby, P., Stadnyk, T.A., Holmes, T., Birks, S.J., Pietroniro, A., 2021. Database of ^{18}O and ^{2}H in streamflow across Canada: a national resource for tracing water sources, water balance and predictive modelling. Data Brief. https://doi.org/10.1016/j.dib.2021.106723.

Gremillion, P., Wanielista, M., 2000. Effects of evaporative enrichment on the stable isotope hydrology of a central Florida (USA) River. Hydrol. Process. 14, 1465–1484.

Halder, J., Terzer, S., Wassenaar, L.I., Araguas-Araguas, L.J., Aggarwal, P.K., 2015. The Global Network of Isotopes in Rivers (GNIR): integration of water isotopes in watershed observation and riverine research. Hydrol. Earth Syst. Sci. Discuss. 19, 3419–3431. https://doi.org/10.5194/hess-19-3419-2015.

Hu, Y., Liu, Z., Zhao, M., et al., 2018. Using deuterium excess, precipitation and runoff data to determine evaporation and transpiration: a case study from the Shawan Test site, Puding, Guizhou, China. Geochim. Cosmochim. Acta 242, 21–33.

Henderson-Sellers, A., McGuffie, K., Noone, D., Irannejad, P., 2004. Using stable water isotopes to evaluate basin-scale simulations of surface water budgets. J. Hydrometeor. 5, 805–822.

Holmes, T.L., Stadnyk, T.A., Kim, S.J., Asadzadeh, M., 2020. Regional calibration with isotope tracers using a spatially distributed model: a comparison of methods. Water Resour. Res. 56 https://doi.org/10.1029/2020WR027447 e2020WR027447.

Horita, J., Wesolowski, D., 1994. Liquid-vapour fractionation of oxygen and hydrogen isotopes of water from the freezing to the critical temperature. Geochim. Cosmochim. Acta 58, 3425–3437. https://doi.org/10.1016/0016-7037(94)90096-5.

Horita, J., Rozanski, K., Cohen, S., 2008. Isotope effects in the evaporation of water: a status report of the Craig-Gordon model. Isot. Environ. Health Stud. 44, 23–49.

IAEA/WMO, 2014. International Atomic Energy Agency/World Meteorological Organization, Global Network of Isotopes in Precipitation. Available at. The GNIP Database, Vienna, Austria. http://www.iaea.org/water.

Jalota, S.K., Prihar, S.S., 1990. Bare-soil evaporation in relation to tillage. Adv. Soil Sci. 12, 187–216.

Jasechko, S., Sharp, Z.D., Gibson, J.J., Birks, S.J., Yi, Y., Fawcett, P.J., 2013. Terrestrial water fluxes dominated by transpiration. Nature 496, 347–350.

Jasechko, S., Sharp, Z.D., Gibson, J.J., Birks, S.J., Yi, Y., Fawcett, P.J., 2014a. Brief communications arising, reply to A. M. J. Coenders-Gerrits et al., uncertainty in evapotranspiration rates. Nature 506, E2–E3. https://doi.org/10.1038/nature12926 (13 February 2014).

Jasechko, S., Gibson, J.J., Edwards, T.W.D., 2014b. Stable isotope mass balance of the North American Great Lakes. J. Great Lakes Res. 40, 336–346. https://doi.org/10.1016/j.jglr.2014.02.020.

Jasechko, S., Kirchner, J.W., Welker, J.M., McDonnell, J.J., 2016. Substantial portion of global streamflow less than three months old. Nat. Geosci. https://doi.org/10.1038/NGEO2636 published online: 18 JANUARY 2016.

Jasechko, S., Wassenaar, L.I., Mayer, B., 2017. Isotopic evidence for widespread cold-season-biased groundwater recharge and young streamflow across central Canada. Ecohydrology 31, 2196–2209. https://doi.org/10.1002/hyp.11175, 2017.

Karim, A., Veizer, J., Barth, J., 2008. Net ecosystem production in the Great Lakes basin and its implications for the North American missing carbon sink: a hydrologic and stable isotope approach. Glob. Planet. Change 61, 15–27.

Kendall, C., Coplen, T.B., 2001. Distribution of oxygen-18 and deuterium in river waters across the United States. Hydrol. Process. 15, 1363–1393.

Kirchner, J.W., 2016. Aggregation in environmental systems – part 1: seasonal tracer cycles quantify young water fractions, but not mean transit times, in spatially heterogeneous catchments. Hydrol. Earth Syst. Sci. Discuss. 20, 279–297. https://doi.org/10.5194/hess-20-279-2016, 2016.

Klaus, J., McDonnell, J.J., 2013. Hydrograph separation using stable isotopes: review and evaluation. J. Hydrol. 505, 47–64. https://doi.org/10.1016/j.jhydrol.2013.09.006.

Koeniger, P., Leibundgut, C., Stichler, W., 2009. Spatial and temporal characterisation of stable isotopes in river water as indicators of groundwater contribution and confirmation of modelling results; a study of the Weser river, Germany. Isotopes Environ. Health Stud. 45 (4), 289–302. https://doi.org/10.1080/10256010903356953.

Kool, D., Ben-Gal, A., Agam, N., Šimůnek, J., Heitman, J., Sauer, T., Lazarovitch, N., 2014. Spatial and diurnal below-canopy evaporation in a desert vineyard: measurements and modeling. Can. Water Resour. J. 50 (8), 7035–7049. https://doi.org/10.1002/2014WR015409.

Kumar, A., Tiwari, S.K., Verma, A., Gupta, A.K., 2018. Tracing isotopic signatures (δD and $\delta^{18}O$) in precipitation and glacier melt over Chorabari Glacier – hydroclimatic inferences for the Upper Ganga Basin (UGB), Garhwal Himalaya. J. Hydrol. 15, 68–89. https://doi.org/10.1016/j.ejrh.2017.11.009.

Lee, D.H., Veizer, J., 2003. Water and carbon cycles in the Mississippi River basin: potential implications for the Northern Hemisphere residual terrestrial sink. Global Biogeochem. Cycles 17 (2), 1037. https://doi.org/10.1029/2002GB001984.

Li, X., Gentine, P., Lin, C., Zhou, S., Sun, Z., Zheng, Y., Liu, J., Zheng, C., 2019. A simple and objective method to partition evapotranspiration into transpiration and evaporation at eddy-covariance sites. Agric. Forest Meteorol. 171–182. https://doi.org/10.1016/j.agrformet.2018.11.017, 2019.

Mastrotheodoros, T., Pappas, C., Molnar, P., Burlando, P., Keenan, T.F., Gentine, P., et al., 2017. Linking plant functional trait plasticity and the large increase in forest water use efficiency. J. Geophys. Res. Biogeosci. 122 (9), 2393–2408.

McDonnell, J.J., 2014. The two water worlds hypothesis: ecohydrological separation of water between streams and trees? WIREs Water 1, 323–329. https://doi.org/10.1002/wat2.1027.

McGuire, K.J., McDonnell, J.J., 2006. A review and evaluation of catchment transit time modeling. J. Hydrol. 330, 543–563.

Mesinger, F., DiMego, G., Kalnay, E., Mitchell, K., Shafran, P.C., Ebisuzaki, W., Jovic, D., Woollen, J., Rogers, E., Berbery, E.H., Ek, M.B., Fan, Y., Grumbine, R., Higgins, W., Li, H., Lin, Y., Manikin, G., Parrish, D., Shi, W., 2006. North American Regional Reanalysis: a long-term, consistent, high-resolution climate dataset for the North American domain, as a major improvement upon the earlier global reanalysis datasets in both resolution and accuracy. Bull. Amer. Meteorol. Soc. 87, 343–360.

Miralles, D.G., Gash, J.H., Holmes, T.R.H., de Jeu, R.A.M., Dolman, A.J., 2010. Global canopy interception from satellite observations. J. Geophys. Res. 115, D16122, 2010.

Muhammad, A., Evenson, G., Stadnyk, T.A., Boulawade, A., Jha, S., Coulibaly, P., 2019. Impact of model structure on the accuracy of hydrological modeling of a Canadian prairie watershed. J. Hydrol Reg. Stud. 21, 40–56.

Nelson, S.T., 2000. A simple, practical methodology for routine VSMOW/SLAP normalization of water samples analyzed by continuous flow methods. Rapid Commun. Mass Spectrom. 14, 1044–1046.

Pang, H., Hou, S., Landais, A., Masson-Delmotte, V., Jouzel, J., Steen-Larsen, H.C., et al., 2019. Influence of summer sublimation on δD, $\delta^{18}O$, and $\delta^{17}O$ in precipitation, East Antarctica, and implications for climate reconstruction from ice cores. J. Geophys. Res. Atmos. 124, 7339–7358. https://doi.org/10.1029/2018JD030218.

Paul, D., Skrzypek, G., 2006. Flushing time and storage effects on the accuracy and precision of carbon and oxygen isotope ratios of sample using the Gasbench II technique. Rapid Commun. Mass Spectrom. 20, 2033–2040. https://doi.org/10.1002/rcm.2559.

Price, J.S., Edwards, T.W.D., Yi, Y., Whittington, P.N., 2009. Physical and isotopic characterization of evaporation from Sphagnum moss. J. Hydrol. 369, 175–182.

Rank, D., Adler, A., Araguas, L.A., Froehlich, K., Rozanski, K., Stichler, W., 1998. Hydrological parameters and climatic signals derived from long term tritium and stable isotopes time-series of the river Danube. Isotope Techniques in the Study of Environmental Change. International Atomic Energy Agency, Vienna, AU, pp. 191–205.

Reckhert, A., Stichler, W., Schmiddt, A., Stumpp, C., 2017. Long-term analysis of stable isotopic composition in German rivers. J. Hydrol. 552, 718–731. https://doi.org/10.1016/j.jgydrol.2017.07.022.

Rodgers, P., Soulsby, C., Waldron, S., Tetzlaff, D., 2005. Using stable isotope tracers to identify hydrological flow paths, residence times and landscape controls in a mesoscale catchment. Hydrol. Earth Syst. Sci. Discuss. 9, 139–155. https://doi.org/10.5194/hess-9-139-2005, 2005.

Schlaepfer, D.R., Ewers, B.E., Shuman, B.N., Williams, D.G., Frank, J.M., Massman, W.J., 2014. Terrestrial water fluxes dominated by transpiration. Ecosphere 5, 1–9. Article 61.

Schleisinger, W.H., Jasechko, S., 2014. Transpiration in the global water cycle. Agric. For. Meteorol. 189-190, 115–117. https://doi.org/10.1016/j.agrformet.2014.01.011.

Schulte, P., Van Geldern, R., Freitag, H., Karim, A., Négrel, P., Petelet-Giraud, E., Probst, A., Probst, J.-L., Telmer, K., Veizer, J., Barth, J.A.C., 2011. Applications of stable water and carbon isotopes in watershed research: weathering, carbon cycling, and water balances. Earth. Rev. 109, 20–31.

Shichun, Z., Xuefa, W., Jianlin, W., Guirui, Y., Xiaomin, S., 2010. The use of stable isotopes to partition evapotranspiration fluxes into evaporation and transpiration. Acta Ecol. Sin. 30, 201–209.

Shook, K., Pomeroy, J., van der Kamp, G., 2015. The transformation of frequency distributions of winter precipitation to spring streamflow probabilities in cold regions; case studies from the Canadian Prairies. J. Hydrol. 521, 394–409. https://doi.org/10.1016/j.jhydrol.2014.12.014, 2015.

Smith, A., Delavau, C., Stadnyk, T., 2015. Identification of geographical influences and flow regime characteristics using regional water isotope surveys in the lower Nelson River, Canada. Can. Water Resour. J. 40, 23–35.

Smith, A., Welch, C., Stadnyk, T., 2016. Assessment of a lumped coupled flow-isotope model in data scarce Boreal catchments. Hydrol. Process. 30 (21), 3871–3884. https://doi.org/10.1002/hyp.10835.

Sokratov, S.A., Golubev, V.N., 2009. Snow isotopic content change by sublimation. J. Glaciol. Geocryol. 193, 823–828.

St. Amour, N.A., Gibson, J.J., Edwards, T.W.D., Prowse, T.D., Pietroniro, A., 2005. Isotopic time-series partitioning of streamflow components in wetland-dominated catchments, lower Liard River Basin, Northwest Territories, Canada. Hydrol. Process. 19, 3357–3381.

Stadnyk, T.A., Holmes, T., 2020. On the value of isotope-enabled hydrologic model calibration. Hydrol. Sci. J. Des Sci. Hydrol. https://doi.org/10.1080/02626667.2020.1751847.

Stadnyk, T.A., Delavau, C.J., Kouwen, N., Edwards, T.W.D., 2013. Towards hydrological model calibration and validation: simulation of stable water isotopes using the isoWATFLOOD model. Hydrol. Processes 27, 3791–3810.

Stadnyk, T.A., Gibson, J.J., Longstaffe, F., 2015. Basin-scale assessment of operational baseflow separation algorithms. J. Hydrol. Eng. 20 (5), 04014074, 2015.

Stadnyk, T.A., Déry, S., MacDonald, M., Koenig, K., 2019. Freshwater system. In: Barber, D., Kuzyk, Z., Candlish, L. (Eds.), An Integrated Regional Impact Assessment of Hudson Bay: Implications of a Changing Environment, pp. 113–153. Québec City, QC, Canada.

Sutanto, S.J., Wenninger, J., Coenders-Gerrits, A.M.J., Uhlenbrook, S., 2012. Partitioning of evaporation into transpiration, soil evaporation and interception: a comparison between isotope measurements and a HYDRUS-1D model. Hydrol. Earth Syst. Sci. Discuss. 16, 2605–2616. https://doi.org/10.5194/hess-16-2605-2012, 2012.

Telmer, K., Veizer, J., 2000. Isotopic constraints on the transpiration, evaporation, energy, and gross primary production budgets of a large boreal watershed: Ottawa River basin, Canada. Global Biogeochem. Cycles 14 (1), 149–165.

Vargas, A.I., Schaffer, B., Yuhong, L., Sternberg, L.S.L., 2017. Testing plant use of mobile vs immobile soil water sources using stable isotope experiments. New Phytol. 215, 582–594. https://doi.org/10.1111/nph.14616.

Vitvar, T., Aggarwal, P.K., Herczeg, A.L., 2007. Global network is launched to monitor isotopes in rivers. Eos Trans. AGU 88 (33), 325. https://doi.org/10.1029/2007EO330001.

Welker, J.M., 2012. ENSO effects on the isotopic ($\delta^{18}O$, $\delta^{2}H$ and d-excess) of precipitation across the US using a long-term network (USNIP). Rapid Commun. Mass Spectrom. 17, 1655–1660. https://doi.org/10.1002/rcm.6298.

Wiken, E.B., 1986. Terrestrial Ecozones of Canada. Ecological Land Classification Series No. 19. Environment Canada, Hull, Que. 26 pp. + map.

Wolfe, J.D., Shook, K.R., Spence, C., Whitfield, C.J., 2019. A watershed classification approach that looks beyond hydrology: application to a semi-arid, agricultural region in Canada. Hydrol. Earth Syst. Sci. Discuss. 23, 3945–3967. https://doi.org/10.5194/hess-23-3945-2019, 2019.